

# Twistronics vs straintronics in twisted bilayer graphene

Marwa Mannaï and Sonia Haddad\*

Laboratoire de Physique de la Matière Condensée,  
Département de Physique, Faculté des Sciences de Tunis,  
Université Tunis El Manar, Campus Universitaire 1060 Tunis, Tunisia

Several numerical studies have shown that the electronic properties of twisted bilayer graphene (TBLG) are tunable by strain engineering of the stacking layers. In particular, the flatness of the low energy moiré bands was found to be, substantially, sensitive to the strain. However, to the best of our knowledge, there is no full analytical calculations of the effect of strain on such bands. We derive, based on the continuum model of Bistritzer and MacDonald [1], the low energy Hamiltonian of the strained TBLG at small twist angles. We obtain the analytical expressions of the strain renormalized Dirac velocities and explain the role of strain in the emergence of the flat bands. We discuss how strain could correct the twist angles and bring them closer to the magic angle  $\theta_m = 1.05^\circ$ . The analytical results are also compared to our numerical tight binding moiré band structure.

*Introduction.* Twistronics has, recently, emerged as a powerful tool to tailor the electronic properties of 2D moiré systems, consisting of accurately stacked two layers of 2D materials with a relative twist angle  $\theta$  [1–13]. The first engineered two layer van der Waals structure is the twisted bilayer graphene (TBLG), which has stimulated extensive theoretical and experimental studies since the discovery of its superconducting state at 1.7K around the so-called, magic angle (MA)  $\theta_m \sim 1.1^\circ$  [14–16]. This discovery has revived hope in unveiling the mechanism of superconductivity in HTC materials, which is one of the long standing puzzles of strongly correlated electrons systems. The origin of superconductivity in TBLG is still under debate, but there is a general consensus on its extreme sensitivity on the occurrence, at the MA, of flat electronic bands, with meV width, located around the charge neutrality point and characterized by a vanishing effective Fermi velocity [17–24]. These flat bands can also emerge in TBLG under small uniaxial heterostrain, of 0.35% at a relative twist angle  $\theta \sim 1.25^\circ$  [25, 26], which opens the way for a strain engineering of flat bands [25]. Strain has also been found to be useful to probe the symmetry of the superconducting order parameter in TBLG [27]. Several experimental and numerical studies have, then, recently focused on the effect of strain on the electronic properties of TBLG and bilayers of transition metal dichalcogenides (TMD) [27–37].

However, a full analytical analysis of the strain dependence of the moiré band structure is still lacking.

In this paper, we derive a low energy effective Hamiltonian of TBLG subject to an heterostrain. We determine the strain dependence of the effective Fermi velocities of the moiré flat bands. We show that, at a given twist angle  $\theta$  away from the MA, it is possible to choose the amplitude and the direction of the strain to flatten the bands around charge neutrality. This result sheds light on the experimental findings reporting a strain induced MA in TBLG at small angle ( $\theta \sim 1.5^\circ$ )

under a moderate heterostrain ( $\epsilon \sim 0.3\%$ ) [26, 30]. Our results may, then, be used to measure the strain tensor components of moiré systems, based on an accurate rotation of the layers. Furthermore, we found that, under a shear strain, the flatness of the moiré bands is only due to the contribution of the strain gauge field  $\mathbf{A}$  to the Dirac point displacements. Our low energy strain dependent Hamiltonian of TBLG may pave the way to a tunable strain moiré bands of 2D bilayer materials.

*Continuum model of strained twisted bilayer graphene:* Under a uniform strain, described by a tensor  $\mathcal{E}$ , and a rotation of small angle  $\theta$ , the low energy Dirac electron Hamiltonian of monolayer graphene (MLG), at a valley  $\xi = \pm$  can be written as [25, 38]:

$$h(\mathbf{k}) = \hbar v_F (\mathbb{I} + \mathcal{E}_t^T - \beta \mathcal{E}) (\mathbf{k} - \mathbf{D}_\xi) \cdot (\xi \sigma_x, \sigma_y) \quad (1)$$

where  $v_F$  is the Fermi velocity of the undeformed layer,  $\sigma$  are the Pauli matrices,  $\mathcal{E}_t = \mathcal{E} + R(\theta)$  is the total deformation tensor including the strain tensor  $\mathcal{E}$  and the small angle rotation matrix  $R(\theta)$  written as:

$$\mathcal{E} = \begin{pmatrix} \epsilon_{xx} & \epsilon_{xy} \\ \epsilon_{xy} & \epsilon_{yy} \end{pmatrix}, \quad R(\theta) = \begin{pmatrix} 0 & -\theta \\ \theta & 0 \end{pmatrix}. \quad (2)$$

$\mathbf{D}_\xi$  is the position of the Dirac points given by [25]:

$$\mathbf{D}_\xi = (\mathbb{I} + \mathcal{E}_t) \mathbf{K}_\xi^0 - \xi \mathbf{A}, \quad (3)$$

$\mathbf{K}_\xi^0 = (\xi \frac{4\pi}{3a}, 0)$  being the Dirac point of the undeformed layer,  $\mathbf{A} = \frac{\sqrt{3}}{2a} \beta (\epsilon_{xx} - \epsilon_{yy}, -2\epsilon_{xy})$  is the effective gauge field,  $\beta \sim 3$  for graphene [39] and  $a$  is the lattice parameter. The  $\beta$  term in Eq.1, which was not included in previous works [25], is due to the strain dependence of the inplane hopping parameters [38]. Actually, our numerical calculations show that this term could be neglected in TBLG regarding the small values of the strain amplitudes reported experimentally and which vary, for uniaxial deformation, from 0.1% to 0.7% [33].

We consider, as in Ref.[25], a homobilayer AA stacking, where the layers (1) and (2) are rotated and strained

in opposite ways with total deformation matrices  $\mathcal{E}_{t2} = -\mathcal{E}_{t1} = \frac{1}{2}\mathcal{E}_t$  where  $\mathcal{E}_t = \mathcal{E}_{t2} - \mathcal{E}_{t1}$  is the relative deformation.

Following the approach of Bistritzer and MacDonald [1] in deriving the low energy continuum model of unstrained TBLG, we write the Hamiltonian of the strained TBLG as [40]:

$$H(\mathbf{k}) = \begin{pmatrix} h_1(\mathbf{k}) & T_1 & T_2 & T_3 \\ T_1^\dagger & h_{2,1}(\mathbf{k}) & 0 & 0 \\ T_2^\dagger & 0 & h_{2,2}(\mathbf{k}) & 0 \\ T_3^\dagger & 0 & 0 & h_{2,3}(\mathbf{k}) \end{pmatrix}, \quad (4)$$

where the corresponding basis  $\Psi = (\psi_0(\mathbf{k}), \psi_1(\mathbf{k}), \psi_2(\mathbf{k}), \psi_3(\mathbf{k}))$  is constructed on the two-component sublattice spinor  $\psi_0(\mathbf{k})$  ( $\psi_j(\mathbf{k})$ ) of layer (1) (layer (2)) taken at the momentum  $\mathbf{k}$  ( $\mathbf{k} + \mathbf{q}_j$ ) around the Dirac point  $D_1$  ( $D_2$ ) at a given valley  $\xi$ .  $h_1$  is the Hamiltonian of the layer (1) written as  $h_1(\mathbf{k}) = \hbar v_F (\mathbb{I} + \mathcal{E}_t^T - \beta\mathcal{E}) \mathbf{k} \cdot (\xi\sigma_x, \sigma_y)$  and  $h_{2,j}$ , ( $j = 1, 2, 3$ ) are those of layer (2) given by  $h_{2,j}(\mathbf{k}) = \hbar v_F (\mathbb{I} + \mathcal{E}_t^T - \beta\mathcal{E}) (\mathbf{k} + \mathbf{q}_j) \cdot (\xi\sigma_x, \sigma_y)$ , where  $\mathbf{k}$  is measured from  $\mathbf{D}_1$ ,  $\mathbf{q}_1 = \mathbf{D}_1 - \mathbf{D}_2 = \mathcal{E}_t^T \mathbf{K}_\xi^0 + \xi\mathbf{A}$ ,  $\mathbf{q}_2 = \mathbf{q}_1 - \mathbf{G}_1^M$  and  $\mathbf{q}_3 = \mathbf{q}_1 - (\mathbf{G}_1^M + \mathbf{G}_2^M)$ . The  $\mathbf{q}_j$ , ( $j = 1, 2, 3$ ) vectors connect the Dirac points  $\mathbf{D}_1$

and  $\mathbf{D}_2$  in the moiré Brillouin zone (BZ) constructed on the basis  $(\mathbf{G}_1^M, \mathbf{G}_2^M)$  given by  $\mathbf{G}_i^M = \mathcal{E}_t^T \mathbf{G}_i$ , where  $\mathbf{G}_1 = \frac{2\pi}{a} (1, -\frac{1}{\sqrt{3}})$ ,  $\mathbf{G}_2 = \frac{2\pi}{a} (0, \frac{2}{\sqrt{3}})$  is the reciprocal lattice basis of undeformed layer.

In the absence of strain, the  $\mathbf{q}_j$  vectors satisfy  $\sum_j \mathbf{q}_j^0 = \mathbf{0}$ ,  $\mathbf{q}_j^0$  denotes the corresponding vectors of the unstrained system. We denote hereafter [40]

$$\mathbf{q}_j = \mathbf{q}_j^0 + \Delta\mathbf{q}_j, \quad (5)$$

where  $\Delta\mathbf{q}_j$  is the strain induced correction.

For an AA layer stacking, the matrices  $T_j$  are given by  $T_1 = w (\mathbb{I} + \sigma_x)$ ,  $T_2 = w (\mathbb{I} - \frac{1}{2}\sigma_x + \frac{\sqrt{3}}{2}\sigma_y)$  and  $T_3 = w (\mathbb{I} - \frac{1}{2}\sigma_x - \frac{\sqrt{3}}{2}\sigma_y)$  [40], where we assumed, for simplicity, that the interlayer tunneling amplitude  $w \sim 110\text{meV}$  is strain independent and that the two layers are unrelaxed [40] as in Ref. [25].

Regarding the small values of the twist angle  $\theta$  and the strain amplitude in TBLG [33], a low energy Hamiltonian  $H^{(1)}(\mathbf{k})$  can be derived from Eq. 4, based on a first order perturbative approach as done in Ref. [1]. To the leading order in  $\mathbf{k}$ ,  $H^{(1)}(\mathbf{k})$  can be written, at the valley  $\xi = +$ , as

$$H^{(1)}(\mathbf{k}) = \frac{\langle \Psi | H(\mathbf{k}) | \Psi \rangle}{\langle \Psi | \Psi \rangle} = \frac{1}{\langle \Psi | \Psi \rangle} \left[ \psi_0^\dagger h_0(\mathbf{k}) \psi_0 + \psi_0^\dagger \sum_j T_j h_j^{-1} h_0(\mathbf{k}) h_j^{-1} T_j^\dagger \psi_0 \right] \quad (6)$$

$\psi_0$  being a zero energy state of the one layer Hamiltonian  $h_0$  (Eq. 1) where the strain and the twist angle could be neglected [1, 40].  $h_j = h_{2,j}(\mathbf{k} = \mathbf{0}) \sim \hbar v_F \sigma \cdot \mathbf{q}_j$ , where the  $\mathbf{q}_j$  are given by Eq. 5 [40].

To the leading order in strain amplitude, the four two-component spinor  $\Psi$  satisfies, as in the unstrained case,  $\langle \Psi | \Psi \rangle \sim 1 + 6\alpha^2$ , where  $\alpha = \frac{w}{\hbar v_F k_\theta}$  and  $k_\theta = 2K^0 \sin \theta/2 \sim \frac{4\pi}{3a}\theta$ ,  $K^0 = \frac{4\pi}{3a}$  being the amplitude of the Dirac point vector of the undeformed layer. The low energy  $2 \times 2$  Hamiltonian given by Eq. 6 reduces, then, to

$$H^{(1)}(\mathbf{k}) = \frac{\hbar}{1 + 6\alpha^2} \psi_0^\dagger [v_{0x} k_x + v_{0y} k_y + \sigma_x v_x k_x + \sigma_y v_y k_y + \sigma_x v_{xy} k_y + \sigma_y v_{yx} k_x] \psi_0 \quad (7)$$

where the tilt parameters  $\mathbf{v}_0 = (v_{0x}, v_{0y})$ , and the strain

renormalized velocities are given by:

$$v_{0x} = -v_F \frac{16\pi}{a} \frac{\alpha^2}{k_\theta} \epsilon_{xy}, \quad v_{0y} = v_F \frac{8\pi}{a} \frac{\alpha^2}{k_\theta} (\epsilon_{yy} - \epsilon_{xx}), \quad v_x = v_F \left( 1 - 3\alpha^2 + \frac{6\sqrt{3}}{a} \frac{\alpha^2}{k_\theta} \beta \epsilon_{xy} \right), \quad v_y = v_F \left( 1 - 3\alpha^2 - \frac{6\sqrt{3}}{a} \frac{\alpha^2}{k_\theta} \beta \epsilon_{xy} \right), \\ v_{xy} = v_F \frac{\alpha^2}{k_\theta} \left[ \left( \frac{4\pi}{3a} - \frac{\sqrt{3}}{a} \beta \right) \epsilon_{xx} + \left( \frac{\sqrt{3}}{a} \beta - \frac{4\pi}{3a} \right) \epsilon_{yy} \right], \quad v_{yx} = v_F \frac{\alpha^2}{k_\theta} \left[ \left( \frac{4\pi}{a} - \frac{3\sqrt{3}}{a} \beta \right) \epsilon_{xx} + \left( \frac{3\sqrt{3}}{a} \beta + \frac{4\pi}{a} \right) \epsilon_{yy} \right] \quad (8)$$

Equations 7 and 8, which are the main results of

the present work, reduce to the expressions obtained by

Bistritzer and MacDonald, in the limit of a vanishing strain[1].

In the Following, we discuss the effect of strain on the flat bands, appearing around the MA  $\theta_m$ .

*Flat band behavior under strain:* According to Eqs. 7 and 8, the flatness of the low energy bands can be selectively tuned by the strain along the moiré BZ directions by choosing, for a given twist angle  $\theta$ , the strain value at which the corresponding effective velocity vanishes. Considering a shear deformation  $\epsilon_{ij \neq i} = \epsilon$ ,  $\epsilon_{ii} = 0$ , the  $v_{0y}$  tilt component and the cross velocity terms  $v_{xy}$  and  $v_{yx}$  turn to zero, while the velocities  $v_x$  and  $v_y$  along, respectively, the  $k_x$  and  $k_y$  axes read as:

$$v_{x,y} = v_0^* + \Delta v_{x,y} \quad (9)$$

where  $v_0^* = \frac{1-3\alpha^2}{1+6\alpha^2}$  is the low energy effective velocity of the unstrained TBLG [1] and the strain induced corrections are

$$\Delta v_{x,y} = \pm \frac{v}{1+6\alpha^2} \frac{\alpha^2 6\sqrt{3}}{k_\theta a} \beta \quad (10)$$

At a twist angle  $\theta = 1.15^\circ$ ,  $v_x$  ( $v_y$ ) vanishes for a compressive (tensile) shear strain of 0.16% amplitude, which is consistent with our numerical tight binding results depicted in Fig.1 (a-d) showing an almost flat band along the  $\Gamma M$  direction of the moiré BZ represented in Figure 1(e).

According to Eq.8, under a compressive (tensile) shear strain  $\epsilon_{xy} < 0$  ( $\epsilon_{xy} > 0$ ), the renormalized velocity  $v_x$  decreases (increases) compared to the unstrained value  $v_0^*$  (Fig.1 (a-d) and (f)). Moreover, the tilt term  $v_{0x}$  deforms the Dirac cone and breaks the particle-hole symmetry. These features are in agreement with the numerical results of Fig.1 (f) showing a deformed Dirac cone at the crossing of the low energy bands around charge neutrality point.

The strain modified Dirac cones shapes could affect the electron-phonon interactions. In monolayer graphene, the strain modified Dirac cone has been found to, particularly, affect the Kohn anomaly [41]. Such anomaly has also been observed in BLG and may, also be, sensitive to strain and twist. This point will be discussed in a forthcoming paper.

The opposite signs of  $\Delta v_{x,y}$ , in Eq.10, is due to the off diagonal structure of the shear strain tensor which is similar to the small twist angle  $R(\theta)$  matrix but with the same sign for both strain tensor components. Therefore, a twist gives rise to an isotropic velocity  $v^* = v_F(1 - 3\alpha^2)/(1+6\alpha^2)$  [1] while a shear strain leads to anisotropic velocities with opposite corrections. It is worth to stress that these corrections are only due to the gauge field  $\mathbf{A}$ . This means that, under a shear strain, the displacement of the Dirac points is the key parameter governing the flatness of the moiré bands.

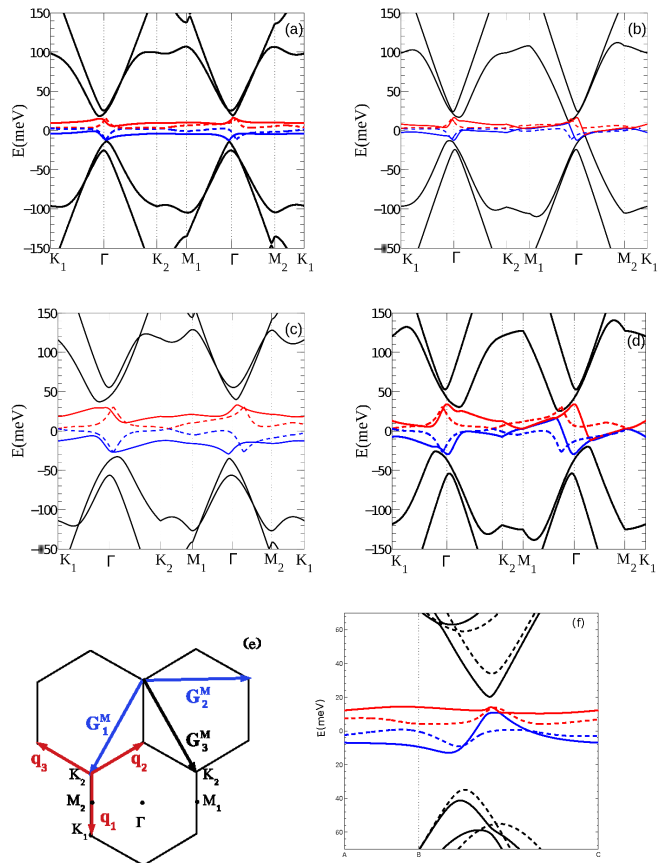


FIG. 1. (a) Low energy band structure of TBLG at twist angles  $\theta = 1.15^\circ$  (upper panels) and  $\theta = 1.25^\circ$  (middle panels) without strain (dashed lines) and under a shear strain (solid lines) of  $-0.16\%$  (a),  $0.16\%$  (b),  $-0.36\%$  (c)  $0.36\%$  (d). The bands are represented along the deformed moiré Brillouin zone along the directions represented, in the unstrained case, in (e). Calculations are done for  $w = 118\text{meV}$  and  $\hbar v_F/a \sim 2.68\text{eV}$  where  $a$  is the lattice parameter of graphene, which corresponds to take  $\theta_m = 1.05^\circ$  for the first MA. The band structures are calculated by diagonalizing the Hamiltonian given by Eq. in the basis of  $\{|\mathbf{k}\rangle_1, |\mathbf{k} + \mathbf{q}_j\rangle_2\}$  constructed by the states around, respectively the Dirac point  $\mathbf{k}_{D1}$  of layer (1) and those in the vicinity of the layer (2) Dirac point  $\mathbf{k}_{D2}$ . A minimum number of 128 states is required to achieve the convergence for the low energy bands. (e) Low energy bands along the  $\mathbf{G}_3^M = \mathbf{G}_1^M + \mathbf{G}_2^M$  and across the  $D_1$  point, where the moiré bands cross. This band structure is obtained for  $\theta = 1.15^\circ$  under a tensile shear strain  $\epsilon_{x,y} = 0.16\%$  and for  $w = 110\text{meV}$  as in Ref.

In Ref.[31], the authors reported, based on DFT calculations that a shear angle  $\gamma \sim 0.08^\circ$  along the armchair direction, introduces a correction of  $\Delta\theta_m = 0.04^\circ$  to the calculated MA,  $\theta_m^{th} = 1.12^\circ$  to agree with the experimental value of  $\theta_m \sim 1.08^\circ$ . This correction can be understood from the expressions of the renormalized velocities given by Eq.8. Let us denote  $\alpha^*$  the corrected value of

$\alpha = \frac{w}{\hbar v_F k_\theta}$  defined by:

$$v_{x,y} = (1 - 3\alpha^2) + \Delta v_{x,y} \equiv v_F (1 - 3\alpha^{*2}), \quad (11)$$

For a twist angle  $\theta_m^{th} = 1.12^\circ$  and a shear strain  $\epsilon \sim \tan \gamma \sim \gamma = 0.14\%$ , and taking  $\hbar v_F/a = 2.68 \text{ eV}$  for graphene [25], we deduce from Eq.11 that the corrected MA ascribed to  $\alpha^*$  is  $\theta^* = 1.04^\circ$ , which is in good agreement with the measured MA of  $1.05^\circ$ .

For a uniaxial strain along the armchair or zigzag directions, the velocity corrections  $\Delta v_{x,y}$  vanishes, which may be used as a probe to check the direction of the applied strain.

Let us consider, as in Ref.[25], a twist angle of  $\theta = 1.05^\circ$  and a uniaxial strain of  $\epsilon = 0.6\%$  applied along the direction  $\varphi = 30^\circ$ . According to Eqs.7 and 8, the corrections to the Dirac velocities reaches  $\pm 0.13v_F$  [40], which agree with the numerical calculations of Ref.[25] where an increase of  $0.14v_F$  was reported.

Based on structural and spectroscopic measurements combined with tight binding calculations, Huder *et al.*[26] showed that flat bands emerge in TBLG under a small uniaxial heterostrain, of the order of  $0.35\%$  and a twist angle of  $\theta = 1.25^\circ$ . Taking  $\theta_m = 1.05^\circ$  as the first MA,  $v_x$  ( $v_y$ ), in Eq.8, vanishes for a uniaxial strain having an off diagonal component  $\epsilon_{xy} = 0.36\%$ , as shown in figure 1 (c), which is consistent with the results of Ref.[26].

The outcomes of the analysis of our results with respect to previous works [25, 31], show that the Hamiltonian given by Eq.7 may provide insights in the behavior of the low energy bands of TBLG under strain.

In conclusion, we derived a low energy Hamiltonian of the TBLG under a strain deformation which captures the interplay between strain and twist and its consequences on the flatness of the moiré bands. We determined the analytical expressions of the strain induced corrections of the effective Fermi velocities. Our results could be used to measure the direction and amplitude of the applied strain, at a given twist angle, or to correct the latter to bring it closer to the MA. The renormalization of the moiré bands by strain may, substantially, affect the electron-electron and the electron-phonon interactions in strained TBLG. The natural question which arises is whether the strain may stabilize the superconducting state in bilayer graphene, twisted at an angle away from the MA. This point is left for further investigations. Moreover, our results can be extended to bilayer of twisted transition metal dichalcogenides where the emergence of the flat band, under strain, is not well understood.

## ACKNOWLEDGMENT

The authors acknowledges the kind hospitality of ICTP (Trieste, Italy) where this work has been started. S. H. was supported by the Simons-ICTP associate fellowship.

\* Electronic address: sonia.haddad@fst.utm.tn

- 
- [1] R. Bistritzer and A. H. MacDonald, Proc. Natl. Acad. Sci.U.S.A., **108**, 12233 (2011).
  - [2] For a review see G. Catarina, B. Amorim, E. V. Castro, J. M. Vi. P. Lopes, N. M. R. Peres, *Handbook of Graphene* Volume 3: *Graphene-like 2D Materials*, Edited by Mei Zhang (John Wiley & Sons, 2019), pp. 177-231, doi:10.1002/9781119468455.ch44
  - [3] For a review see A. Nimbalkar, H. K. Nano-Micro Lett. **12**, 126 (2020).
  - [4] J. M. B. Lopes dos Santos, N. M. R. Peres, and A. H. Castro Neto, Phys. Rev. Lett. **99**, 256802 (2007).
  - [5] M. Koshino, P. Moon, J. Phys. Soc. Jpn. **84**, 121001 (2015).
  - [6] D. Weckbecker, S. Shallcross, M. Fleischmann, N. Ray, S. Sharma, and O. Pankratov, Phys. Rev. B **93**, 035452 (2016).
  - [7] K. Kim, A.DaSilva, S. Huang, B. Fallahazad, S. Larentis, T. Taniguchi, K. Watanabe, B. J. LeRoy, A. H. MacDonald, and E.Tutuc, Proc. Natl. Acad. Sci.U.S.A., **114**, 3364(2017).
  - [8] M. Koshino, N. F. Q. Yuan, T. Koretsune, M. Ochi, K. Kuroki, and L. Fu, Phys. Rev. X **8**, 031087 (2018).
  - [9] X. Lin and D. Tománek, Phys. Rev. B **98**, 081410(R) (2018).
  - [10] D. Marchenko, D. V. Evtushinsky, E. Golias, A. Varykhalov, Th. Seyller and O. Rader, Sci. Adv. **4**, eaau0059 (2018).
  - [11] G.Tarnopolsky, A. J.Kr uchkov, and A. Vishwanath, Phys. Rev. Lett. **122**, 106405 (2019).
  - [12] L. Balents, SciPost Phys. **7**, 048 (2019).
  - [13] Z. Zhu , S. Carr, D. Massatt, M.Luskin, and E. Kaxiras, Phys. Rev. Lett. **125**, 116404 (2020).
  - [14] Y. Cao, V. Fatemi, S. Fang, K. Watanabe, T. Taniguchi, E. Kaxiras, and P. Jarillo-Herrero, Nature, **556**, 43 (2018).
  - [15] Y. Cao, V. Fatemi, A. Demir, S. Fang, S. L. Tomarken, J. Y. Luo, J. D. Sanchez-Yamagishi, K. Watanabe, T. Taniguchi, E. Kaxiras, R. C. Ashoori, and P. Jarillo-Herrero, Nature, **556**, 80 (2018).
  - [16] M. Yankowitz, S. Chen, H. Polshyn, Y. Zhang, K. Watanabe, T. Taniguchi, D. Graf, A. F. Young, C. R. Dean, Science **363**, eaav1910 (2019).
  - [17] N. B. Kopnin, T. T. Heikkila, and G. E. Volovik, Phys. Rev. B **83**, 220503(R) (2011).
  - [18] H. C. Po, L. Zou, A. Vishwanath, and T. Senthil, Phys. Rev. X **8**, 031089 (2018).
  - [19] F. Wu, A. H. MacDonald, and I. Martin, Phys. Rev. Lett. **121**, 257001 (2018).
  - [20] B. Roy and V. Juricic, Phys. Rev. B **99**, 121407(R) (2019).

- [21] B. Lian, Z. Wang, and B. A. Bernevig, Phys. Rev. Lett. **122**, 257002 (2019).
- [22] P. Stepanov, I. Das, X. Lu, A. Fahimniya, K. Watanabe, T. Taniguchi, F. H. L. Koppens, J. Lischner, L. Levitov and D. K. Efetov, Nature **583**, 375 (2020).
- [23] Y. Saito, J. Ge, K. Watanabe, T. Taniguchi, A. F. Young, Nature Physics **16**, 926 (2020).
- [24] Y. Cao, D. Rodan-Legrain, J. M. Park, F. N. Yuan, K. Watanabe, T. Taniguchi, R. M. Fernandes, L. Fu, P. Jarillo-Herrero, arXiv:2004.04148 (unpublished).
- [25] Z. Bi, N. F. Q. Yuan and L. Fu, Phys. Rev. B **100**, 035448 (2019).
- [26] L. Huder, A. Artaud, T. Le Quang, G. Trambly de Laisardière, A. G. M. Jansen, G. Lapertot, C. Chapelier, and V. T. Renard, Phys. Rev. Lett. **120**, 156405 (2018).
- [27] F. Wu and S. Das Sarma, Phys. Rev. B **99**, 220507(R) (2018).
- [28] W. Yan, W.-Y. He, Z.-D. Chu, M. Liu, L. Meng, R.-F. Dou, Y. Zhang, Z. Liu, J.-C. Nie and L. He, Nat Commun **4**, 2159 (2013).
- [29] V. H. Nguyen and P. Dollfus, 2D Mater. **2** 035005 (2015).
- [30] J.-B. Qiao, L.-J. Yin and L. He, Phys. Rev. B **98**, 235402 (2018).
- [31] X. Lin, D. Liu and D. Tománek, Phys. Rev. B **98**, 195432 (2018).
- [32] H. Shi, Z. Zhan, Z. Qi, K. Huang, E. van Veen, J. A. Silva-Guillén, R. Zhang, P. Li, K. Xie, H. Ji, M. I. Katsnelson, S. Yuan, S. Qin, Z. Zhang, Nat Commun. **11**, 371 (2020).
- [33] A. Kerelsky, L. J. McGilly, D. M. Kennes, L. Xian, M. Yankowitz, S. Chen, K. Watanabe, T. Taniguchi, J. Hone, C. Dean, A. Rubio and A. N. Pasupathy, Nature **572**, 95 (2019).
- [34] P. A. Pantaleon, T. Low, F. Guinea, arXiv:2010.11086 (unpublished).
- [35] C.-P. Zhang, J. Xiao, B. T. Zhou, J.-X. Hu, Y.-M. Xie, B. Yan, K. T. Law, arXiv:2010.08333 (unpublished).
- [36] N.P. Kazmierczak, M. Van Winkle, C. Ophus, K. C. Bustillo, H. G. Brown, S. Carr, J. Ciston, T. Taniguchi, K. Watanabe, D. K. Bediako, arXiv:2008.09761 (unpublished).
- [37] Y. Zhang, Z. Hou, Y.-X. Zhao, Z.-H. Guo, Y.-W. Liu, S.-Y. Li, Y.-N. Ren, Q.-F. Sun, and L. He Phys. Rev. B **102**, 081403(R) (2020)
- [38] M. Oliva-Leyva and G. G. Naumis, Phys. Rev. B **88**, 085430 (2013), M. Oliva-Leyva and C. Wang, J. Phys.: Condens Matter **29**, 165301 (2017).
- [39] N. N. T. Nam and M. Koshino, Phys. Rev. B **96**, 075311 (2017).
- [40] See Supplementary Material for the details of the continuum model of TBLG under strain.
- [41] S. Haddad and L. Mandhour, Phys. Rev. B **98**, 115420 (2018).

## Supplementary material for Twistronics *vs* straintronics in twisted bilayer graphene

### DERIVATION OF THE LOW ENERGY HAMILTONIAN OF STRAINED TBLG

To derive the low energy Hamiltonian of unstrained TBLG, Bistritzer and MacDonald [1] considered the leading terms in the interlayer tunneling amplitude, which reduce to three nearest hopping processes in momentum space connecting states  $|\mathbf{k}\rangle_1$  around the Dirac point  $\mathbf{k}_{D1}$  of layer (1) to the states  $|\mathbf{k} + \mathbf{q}_j\rangle_2$  around  $\mathbf{k}_{D2}$ , the Dirac point of layer (2). The  $\mathbf{q}_j$  vectors are given by

$$\begin{aligned}\mathbf{q}_1 &= k_\theta (0, -1), \quad \mathbf{q}_2 = \mathbf{q}_1 - \mathbf{G}_1^M = k_\theta \left( \frac{\sqrt{3}}{2}, \frac{1}{2} \right), \\ \mathbf{q}_3 &= \mathbf{q}_1 - (\mathbf{G}_1^M + \mathbf{G}_2^M) = k_\theta \left( -\frac{\sqrt{3}}{2}, \frac{1}{2} \right),\end{aligned}\tag{12}$$

where  $k_\theta = 2k_D \sin \frac{\theta}{2}$  and  $k_D = |\mathbf{k}_{D1}| = |\mathbf{k}_{D2}| = \frac{4\pi}{3a}$ ,  $a$  being the graphene lattice parameter. The  $(\mathbf{G}_1^M, \mathbf{G}_2^M)$  is the moiré BZ basis (Fig.1(e) given by [25]:  $\mathbf{G}_i^M = \mathcal{E}_t^T \mathbf{G}_i$ ,  $\mathcal{E}_t$  being the total deformation tensor,  $\mathbf{G}_i$  are the lattice basis vectors of the monolayer reciprocal lattice  $\mathbf{G}_1 = \frac{2\pi}{a} \left( 1, \frac{-1}{\sqrt{3}} \right)$  and  $\mathbf{G}_2 = \frac{2\pi}{a} \left( 0, \frac{2}{\sqrt{3}} \right)$ . The Dirac point of a layer satisfies  $\mathbf{k}_{D1} = \xi \frac{1}{3} (2\mathbf{G}_1 + \mathbf{G}_2)$ , which leads to  $\sum_{j=1}^3 \mathbf{q}_j = \mathbf{0}$  for the unstrained TBLG.

In the basis  $\{|\mathbf{k}\rangle_1, |\mathbf{k} + \mathbf{q}_j\rangle_2\}$ , the Hamiltonian, at the valley  $\xi = +$ , reads as [1]

$$H(\mathbf{k}) = \begin{pmatrix} h_1(\mathbf{k}) & T_1 & T_2 & T_3 \\ T_1^\dagger & h_2(\mathbf{k} + \mathbf{q}_1) & 0 & 0 \\ T_2^\dagger & 0 & h_2(\mathbf{k} + \mathbf{q}_2) & 0 \\ T_3^\dagger & 0 & 0 & h_2(\mathbf{k} + \mathbf{q}_3) \end{pmatrix},\tag{13}$$

For the relaxed TBLG the  $T_i$  matrices are given by [8]:

$$T_1 = \begin{pmatrix} w & w' \\ w' & w'' \end{pmatrix}, T_2 = e^{i\mathbf{G}_1^M \cdot \mathbf{r}} \begin{pmatrix} w & w'e^{-i\Phi} \\ w'e^{i\Phi} & w'' \end{pmatrix}, T_3 = e^{i(\mathbf{G}_1^M + \mathbf{G}_2^M) \cdot \mathbf{r}} \begin{pmatrix} w & w'e^{i\Phi} \\ w'e^{i\Phi} & w'' \end{pmatrix}, \quad (14)$$

where  $\mathbf{r}$  is the relative shift between the layers, which does not affect the energy spectrum and can be set to  $\mathbf{r} = \mathbf{0}$ [1].  $\Phi = \frac{2\pi}{3}$  and the  $w$ ,  $w'$  and  $w''$  are the tunneling amplitudes which should depend on strain. However, for a seek of simplicity, we assume that, to the leading order in strain, the tunneling amplitudes are strain independent and we consider, as in Ref.[25], unrelaxed layers with  $w = w' = w'' \sim 110\text{meV}$ . In Eq.13,  $h_1(\mathbf{k}) = \hbar v_F (\sigma_x, \sigma_y) \cdot \mathbf{k}$  is the Hamiltonian of layer (1) in the vicinity of the Dirac point  $\mathbf{k}_{D1}$ , while  $h_2(\mathbf{k}_j) = h_2(\mathbf{k} + \mathbf{q}_j)$  is that of layer (2) around  $\mathbf{K}_{D2}$ , where the momentum  $\mathbf{k}$  is written relatively to  $\mathbf{k}_{D1}$ .

The  $\mathbf{k}$  dependent term in Eq.13 is treated as a perturbation and to the leading order in  $\mathbf{k}$ , the effective Hamiltonian can be written as

$$H^{(1)}(\mathbf{k}) = \frac{\langle \Psi | H(\mathbf{k}) | \Psi \rangle}{\langle \Psi | \Psi \rangle}, \quad (15)$$

where  $\Psi = (\psi_0(\mathbf{k}), \psi_1(\mathbf{k}), \psi_2(\mathbf{k}), \psi_3(\mathbf{k}))$  is the zero energy eigenstate of  $H(\mathbf{k} = \mathbf{0})$ .  $\Psi$  is constructed on the two-component sublattice spinor  $\psi_0(\mathbf{k})$  ( $\psi_j(\mathbf{k})$ ) of layer (1) (layer (2)) taken at the momentum  $\mathbf{k}$  ( $\mathbf{k} + \mathbf{q}_j$ ) around the Dirac point  $\mathbf{k}_{D1}$  ( $\mathbf{k}_{D2}$ ) at a given valley  $\xi$ . The  $\Psi$  components satisfy :

$$h_1\psi_0 + \sum_j T_j\psi_j = 0, \{\text{and } T_j^*\psi_0 + h_j\psi_j = 0, \quad (16)$$

where  $h_j \equiv h_2(\mathbf{q}_j)$ . Since  $\psi_0$  is the zero energy eigenstate of  $h_1$ , then:

$$\psi_j = -h_j^{-1}T_j^*\psi_0, \text{ and } \sum_j T_j h_j^{-1}T_j^* = 0. \quad (17)$$

To the leading order in  $\mathbf{k}$ , and neglecting  $\theta$  in  $h_j$  and  $h_1$  [1],  $H^{(1)}(\mathbf{k})$ , takes the following form:

$$H^{(1)}(\mathbf{k}) = \frac{\langle \Psi | H(\mathbf{k}) | \Psi \rangle}{\langle \Psi | \Psi \rangle} = \frac{1}{\langle \Psi | \Psi \rangle} \left[ \psi_0^\dagger h_1(\mathbf{k}) \psi_0 + \psi_0^\dagger \sum_j T_j h_j^{-1} h_1(\mathbf{k}) h_j^{-1} T_j^\dagger \psi_0 \right] = \psi_0^\dagger v^* \sigma \cdot \mathbf{k}, \quad (18)$$

where  $v^* = \frac{1-3\alpha^2}{1+6\alpha^2}$ .

In the strained TBLG, the Hamiltonian of layer ( $i$ ) rotated at a small angle  $\theta_i$  and subject to a strain tensor  $\epsilon_i$  is written as:

$$h_1(\mathbf{k}) = \hbar v_F \sigma \cdot (\mathbb{I} + \mathcal{E}_{t1} - \beta\epsilon_1) \mathbf{k} \\ h_2(\mathbf{k}) = \hbar v_F \sigma \cdot (\mathbb{I} + \mathcal{E}_{t2} - \beta\epsilon_2) (\mathbf{k} + \mathbf{q}_j) \quad (19)$$

where  $\mathcal{E}_{ti} = \epsilon_i + R(\theta_i)$  is the total deformation tensor and  $R(\theta_i)$  is the rotation matrix.

Now, the  $\mathbf{q}_j$  vectors connect the Dirac point  $\mathbf{k}_{D1}$ , of layer (1) to the neighboring  $\mathbf{k}_{D2}$  points, of layer (2) for which the interlayer tunneling amplitudes are the most dominant. Taking into account the displacement of the Dirac points under strain (Eq.3),  $\mathbf{q}_j$  takes the form:

$$\mathbf{q}_1 = \mathbf{k}_{D1} - \mathbf{k}_{D2} = \mathcal{E}_t^T \mathbf{k}_0^\xi + \xi \mathbf{A}, \mathbf{q}_2 = \mathbf{q}_1 - \mathbf{G}_1^M, \mathbf{q}_3 = \mathbf{q}_1 - (\mathbf{G}_1^M + \mathbf{G}_2^M) \quad (20)$$

As in Ref.[1], the unperturbed Hamiltonian, corresponds to  $\mathbf{k} = \mathbf{0}$ , then the  $h_j$  terms read as:  $h_j = \hbar v_F \sigma \cdot \mathbf{Q}_j$  where  $\mathbf{Q}_j = (\mathbb{I} + \mathcal{E}_t - \beta\epsilon) \mathbf{q}_j$ . To the first order in strain, we set  $\mathbf{Q}_j \sim \mathbf{q}_j$  and  $\mathbf{q}_j = \mathbf{q}_j^0 + \Delta \mathbf{q}_j$ , where  $\mathbf{q}_j^0$  correspond to vectors of the unstrained TBLG given by Eq.12.

The amplitude of the four two-component spinor  $\Psi$  is  $\langle \Psi | \Psi \rangle = |\psi_0|^2 + \sum_j |\psi_j|^2$  with  $\psi_j$  given by Eq.17 where  $h_j^{-1} = -\frac{1}{\hbar v_F |\mathbf{q}_j|^2} \sigma \cdot \mathbf{q}_j$ . To the leading term in strain,  $\Psi$  amplitude is unchanged compared to the unstrained case  $\langle \Psi | \Psi \rangle \sim 1 + 6\alpha^2$ .

To the first order in  $\mathbf{k}$ , the effective Hamiltonian becomes:

$$H^{(1)}(\mathbf{k}) = \frac{\langle \Psi | H(\mathbf{k}) | \Psi \rangle}{\langle \Psi | \Psi \rangle} = \frac{1}{\langle \Psi | \Psi \rangle} \left[ \psi_0^\dagger h_0(\tilde{\mathbf{k}}) \psi_0 + \psi_0^\dagger \sum_j T_j h_j^{-1} h_0(\tilde{\mathbf{k}}) h_j^{-1} T_j^\dagger \psi_0 \right], \quad (21)$$

where  $\tilde{\mathbf{k}} = (\mathbb{I} + \mathcal{E}_t - \beta\epsilon) \mathbf{k}$ .

To the lowest order in strain, the Hamiltonian  $H^{(1)}$  reduce to Eq.7, where the tilt parameter  $\mathbf{v}_0 = (v_{0x}, v_{0y})$  and renormalized velocities are given by

$$\begin{aligned} v_{0x} &= 2v_F \frac{\alpha^2}{k_\theta} \left[ \Delta q_{3y} + \Delta q_{2y} - 2\Delta q_{1y} + \sqrt{3}(\Delta q_{3x} - \Delta q_{2x}) \right], v_{0y} = 2v_F \frac{\alpha^2}{k_\theta} \left[ \Delta q_{3x} + \Delta q_{2x} - 2\Delta q_{1x} + \sqrt{3}(\Delta q_{2y} - \Delta q_{3y}) \right], \\ v_x &= v_F \left[ 1 - 3\alpha^2(1 + (1 - \beta)\epsilon_{xx}) \right] + \frac{v_F \alpha^2}{k_\theta} \left[ -\Delta q_{3y} - \Delta q_{2y} - 4\Delta q_{1y} + \sqrt{3}(\Delta q_{2x} - \Delta q_{3x}) \right], \\ v_y &= v_F \left[ 1 - 3\alpha^2(1 + (1 - \beta)\epsilon_{yy}) \right] + \frac{v_F \alpha^2}{k_\theta} \left[ 3(\Delta q_{3y} + \Delta q_{2y}) + \sqrt{3}(\Delta q_{2x} - \Delta q_{3x}) \right], \\ v_{xy} &= -3v_F \alpha^2 [\theta + (1 - \beta)\epsilon_{xy}] + \frac{v_F \alpha^2}{k_\theta} \left[ -(\Delta q_{3x} + \Delta q_{2x}) + \sqrt{3}(\Delta q_{3y} - \Delta q_{2y}) \right], \\ v_{xy} &= -3v_F \alpha^2 [(1 - \beta)\epsilon_{xy} - \theta] + \frac{v_F \alpha^2}{k_\theta} \left[ -3(\Delta q_{3x} + \Delta q_{2x}) + \sqrt{3}(\Delta q_{2y} - \Delta q_{3y}) \right], \end{aligned} \quad (22)$$

The  $\Delta \mathbf{q}_j$  read as

$$\begin{aligned} \Delta \mathbf{q}_1 &= \left( \frac{4\pi}{3a} \epsilon_{xx} + A_x, \frac{4\pi}{3a} \epsilon_{xy} + A_y \right), \text{ where } \mathbf{A} = \frac{\sqrt{3}}{2a} \beta (\epsilon_{xx} - \epsilon_{yy}, -2\epsilon_{xy}) \\ \Delta \mathbf{q}_2 &= \left( \Delta q_{1x} - \frac{2\pi}{a} \left( \epsilon_{xx} - \frac{1}{\sqrt{3}} \epsilon_{xy} \right), \Delta q_{1y} - \frac{2\pi}{a} \left( \epsilon_{xy} - \frac{1}{\sqrt{3}} \epsilon_{yy} \right) \right), \\ \Delta \mathbf{q}_3 &= \left( \Delta q_{1x} - \frac{2\pi}{a} \left( \epsilon_{xx} + \frac{1}{\sqrt{3}} \epsilon_{xy} \right), \Delta q_{1y} - \frac{2\pi}{a} \left( \epsilon_{xy} + \frac{1}{\sqrt{3}} \epsilon_{yy} \right) \right), \end{aligned} \quad (23)$$

At small angle, one can neglect, in Eq.22, the correction terms of the form  $\epsilon_{ij}(1 - \beta)$  and  $\epsilon_{ij}(1 - \beta) - \theta$  compared to  $\frac{\Delta q_j}{k_\theta} \sim \frac{\epsilon_{ij}}{\theta}$ . The expressions given by Eq.22 lead to those of Eq.8.